



# Research on Obstacle Avoidance Tracking Planning of Hyper-redundant Manipulator Based on VR Technology

Xiao-zheng Wan<sup>1(✉)</sup>, Song Zhang<sup>2</sup>, Ji-ming Zhang<sup>1</sup>, Hui Chai<sup>1</sup>,  
and Dong-bao Ma<sup>3</sup>

<sup>1</sup> Institute of Oceanographic Instrumentation, Qilu University of Technology  
(Shandong Academy of Sciences), Qingdao 266061, China  
wanxzz302@outlook.com

<sup>2</sup> College of New Energy, China University of Petroleum,  
Qingdao 266580, China

<sup>3</sup> College of Mechatronic Engineering,  
Beijing Polytechnic, Beijing 100176, China

**Abstract.** In order to ensure that the super-redundant manipulator can work without collision in the obstacle space, this paper designs an obstacle avoidance trajectory planning method for the super-redundant manipulator based on VR technology. The super-redundant manipulator with seven degrees of freedom was selected as the research object, VR technology was introduced to construct the virtual model of the super-redundant manipulator, and the redundancy space of the manipulator was determined according to the model. Then, the pre-selected minimum distance index is selected as the obstacle avoidance index of the mechanical arm. Based on the calculated real-time minimum distance, the inverse kinematics equation of the mechanical arm is obtained by using the escape velocity dynamic obstacle avoidance algorithm, so as to realize the tracking planning of the obstacle avoidance trajectory of the super-redundant mechanical arm. Simulation experiment results show that: it can be seen from the curve of the joint Angle and angular velocity of the manipulator that the proposed method successfully avoided obstacles and reached the target configuration after the application of the proposed method, which met the requirements of the obstacle-avoidance trajectory tracking planning of the current hyperredundant manipulator, and fully proved the effectiveness of the proposed method.

**Keywords:** VR technology · Super redundant manipulator · Obstacle avoidance trajectory planning · Inverse kinematic equation of mechanical arm

## 1 Introduction

As a kind of joint mechanical device simulating the human arm, the mechanical arm has developed into the supporting technology of modern high-end manufacturing industry, and has been widely used in many fields such as material welding, spraying, handling, cutting and so on. Through the operation of the manipulator arm, not only the

production efficiency and operation quality is improved, but also the existing labor environment is improved, so that it can gradually replace the manual operation in high-risk environment [1]. With the continuous expansion of production requirements, the operating environment of manipulator in many application fields is no longer a relatively free space, but a constrained space formed by many obstacles. Therefore, the obstacle avoidance planning of manipulator has become one of the important research directions in the technical field of manipulator [2].

For hyperredundant manipulator, the number of degrees of freedom of the joints is greater than the degree of freedom limited by the end-effector pose. Each joint can move from an initial joint position to the desired joint position in joint space without changing the end-effector position (pose). Because of this feature, the hyperredundant manipulator improves the joint configuration of the low-DOF manipulator and overcomes the shortcomings of the general manipulator, such as poor flexibility, low obstacle avoidance ability, joint overrun and poor dynamic performance, which has become the focus of people's attention.

The redundancy of the hyperredundant manipulator brings difficulties to its inverse motion process. One pose of the hyperredundant manipulator corresponds to numerous joint configurations, and how to choose from the numerous configurations becomes a difficulty. When hyperredundant manipulator moves in free space, trajectory tracking planning can be accomplished by using inverse kinematics. However, when the hyperredundant manipulator moves in the obstacle space, it is very important to plan a collision free trajectory for the safety of the hyperredundant manipulator and other equipment in the space.

At present, relevant scholars have designed a series of obstacle avoidance trajectory planning methods for manipulator, such as the obstacle avoidance trajectory tracking planning method for hyperredundant manipulator based on particle swarm optimization algorithm and the obstacle avoidance trajectory tracking planning method for hyperredundant manipulator based on multi-objective ant colony algorithm, etc. However, in practical application, it is found that the ideal degree of application effect of the above traditional methods is low. Therefore, this paper proposes an obstacle avoidance trajectory planning method of super redundant manipulator based on VR technology. The design idea of the new method is as follows:

- (1) Taking the 7-DOF hyperredundant manipulator as the research object, the virtual model of the hyperredundant manipulator was constructed by VR technology, and the redundant space of the manipulator was determined according to the constructed model.
- (2) The pre-selected minimum distance index was selected as the obstacle avoidance index of the manipulator, and the real-time minimum distance was calculated. Then, the inverse kinematics equation of the manipulator was established by using the escape velocity dynamic obstacle avoidance algorithm, so as to realize the tracking planning of the obstacle avoidance trajectory of the hyperredundant manipulator.

## 2 Research on Tracking Planning Method of Obstacle Avoidance Trajectory Information of Hyper-redundant Manipulator

### 2.1 Introduction of VR Technology

Due to the human participation, in the past, the accuracy of the obstacle avoidance trajectory planning process of super redundant manipulator is very low, which only uses the naked eye to observe the target. It is high precision and inflexible to solve the problem by machine. According to the data given by the computer, the operator's operation mode combines the advantages of the two well, and VR technology can realize the good combination of the two [3].

In order to facilitate the operator to observe the video scene, the virtual model is drawn in wireframe mode, as shown in Fig. 1.

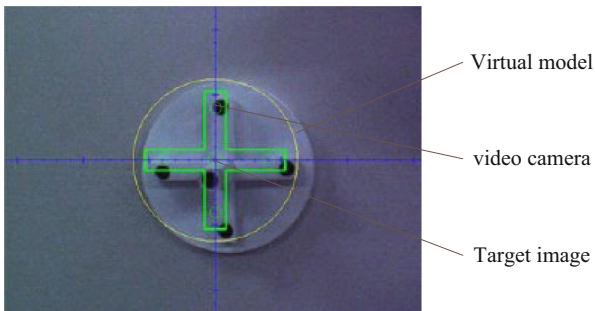


**Fig. 1.** Superposition of target image and virtual model

The video image is captured by the camera carried by the end of the manipulator. The virtual model represents the state that the manipulator moves to the target position accurately, that is, the state that the target and its mark point should move to when it can grab the position of the replaceable module [4].

The camera used in this paper is the industrial camera produced by point grey company, the model is FL2-03S2C, the resolution is  $640 \times 480$ , the lens is 09C Industrial lens of computer company, the field of view is  $32^\circ$ .

### 2.2 Build a Virtual Model of the Robotic Arm

A seven-degree-of-freedom super-redundant manipulator is selected as the research object, which is composed of seven joints, two end effectors, and two arm rods. Its structure is shown in Fig. 2.

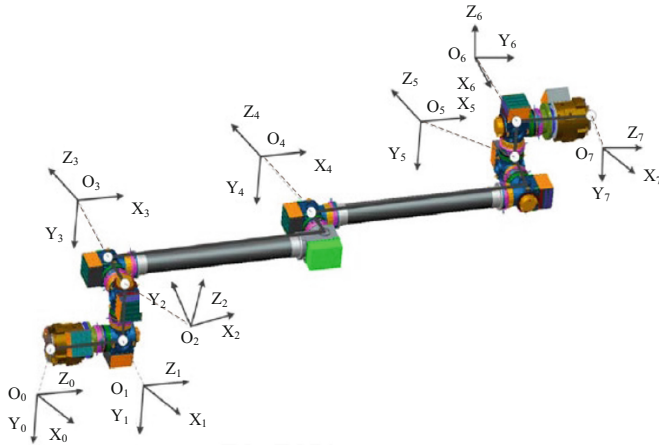


**Fig. 2.** Three-dimensional model and coordinate system of a seven-degree-of-freedom super-redundant manipulator

Adopt the degree of freedom configuration of  $R\perp R\parallel R\perp R$ ,  $R$  represents the rotation joint,  $\perp$  represents the axis of the two joints are perpendicular to each other,  $\parallel$  represents the axis of the two joints are parallel to each other. There is an end effector at each end of the robotic arm, and one end effector is used to connect the robotic arm to the space station and serves as the working base of the robotic arm. The other end effector serves as a tool for the robotic arm to capture operations. The base and end functions of the robotic arm are fully reused, so that the robotic arm has a “crawling” function and increases the operating space. Seven degrees of freedom at the same time, the super redundancy configuration, not only can be done using redundant features from the singular, obstacle avoidance, joint torque optimization task, increase the mechanical arm operation flexibility, but also can be used as a backup technology, in the case of a joint failure of mechanical arm, the rest of the six joints still can complete the task of three dimensional space [5].

The virtual model of the robotic arm is established according to the coordinate system of Fig. 1, and the corresponding D-H parameters are shown in Table 1.

**Table 1.** D-H parameter table of virtual model of robotic arm

$i$	$\theta_i$ ( $^\circ$ )	$d_i$ (mm)	$a_{i-1}$ (mm)	$\alpha_{i-1}$ ( $^\circ$ )
1	0	$a_0$	0	0
2	90	$a_1$	0	90
3	0	$a_2$	0	-90
4	0	$a_4$	$a_3$	0
5	0	$a_6$	$a_5$	0
6	-90	$a_7$	0	90
7	0	$a_8$	0	-90

The transformation matrix of 7-DOF super redundant manipulator is as follows:

$${}^0_7T = {}^0_1T_1{}^1_2T_2{}^2_3T_3{}^3_4T_4{}^4_5T_5{}^5_6T_6{}^6_7T_7 \tag{1}$$

Equation (1) represents the forward kinematics model of the robotic arm, and establishes the mapping relationship between the operating space and the joint space. From this formula, the pose transformation from the 7th coordinate system to the base coordinate system  $O_0 - x_0y_0z_0$  can be obtained.

The core problem of hyper-redundant manipulator kinematics is inverse kinematics. Assuming the end pose (task space)  $X = [x_1, x_2, \dots, x_m]$ , joint space  $\theta = [\theta_1, \theta_2, \dots, \theta_n]$ ,  $n > m$  of the hyper-redundant manipulator, there are:

$$X = f(\theta) \tag{2}$$

In formula (2),  $f(\bullet)$  represents the mapping function from joint space to task space, that is, the positive kinematics equation. Knowing the value of each joint variable, the pose of the end can be uniquely determined. When the end pose is known, solving the value of each joint variable is an inverse kinematics problem [6]. Since the dimension of the joint space is greater than the dimension of the task space, the inverse kinematics is solved directly, and the same pose corresponds to an infinite number of configurations. Therefore, it is necessary to supplement appropriate constraints to make the inverse kinematics of the hyper-redundant manipulator have a unique solution. This is the difficulty of the inverse kinematics of the super-redundant manipulator, and it is also the advantage of the super-redundant manipulator. It can improve the working quality of the manipulator or achieve other goals by supplementing appropriate constraints.

Most of the inverse kinematics of hyper-redundant manipulators are solved by velocity-based methods. Knowing the joint velocity  $\dot{\theta}$  and the Jacobian matrix  $J \in \mathbb{R}^{m \times n}$ , the end pose velocity  $\dot{X} = J\dot{\theta}$  can be obtained. Velocity-based inverse kinematics is the inverse process of the above process, that is, given the pose velocity  $\dot{X}$ , the joint velocity  $\dot{\theta}$  is solved, and the joint angle is obtained by integrating the joint velocity. For the hyper-redundant manipulator, under the condition of full rank of the Jacobian matrix,  $\dot{\theta} = J^{-1}\dot{X}$ ; but because the Jacobian matrix of the hyper-redundant manipulator is not a square matrix, its inverse value cannot be calculated.

The scholar Whitney first proposed the pseudo-inverse method to solve the inverse kinematics of the hyper-redundant manipulator. In essence, it is an optimization problem as follows:

$$\begin{cases} \min \|\dot{\theta}\| \\ \text{subject to: } \min \|\dot{X} - J\dot{\theta}\| \end{cases} \tag{3}$$

Equation (3) shows that the norm of joint velocity should be minimized on the premise of minimum error of end tracking trajectory, so the solution obtained by pseudo inverse method is also called minimum norm solution. The Lagrange multiplier method is used to solve the optimization problem of Eq. (3):

$$\dot{\theta} = J^+ \dot{X} \tag{4}$$

In Eq. (4),  $J^+$  represents the pseudo inverse of Jacobian matrix.

### 2.3 Determine the Redundant Space of Manipulator

The redundancy space of the robot arm greatly affects the accuracy of obstacle avoidance trajectory tracking planning. Therefore, the determination of the redundancy space of the robot arm is studied in this paper.

For the hyper-redundant manipulator, the Jacobian matrix  $J$  is a rectangular matrix. If the rank  $r = m$  of the Jacobian matrix, the column space of the Jacobian matrix is the entire  $R^m$  space. For any end velocity  $\dot{X}$ , the Eqs. (5) has an infinite number of feasible solutions  $\dot{\theta}$ , and redundancy refers to the uncertainty of Eq. (5). Assuming that  $\dot{\theta}_s$  is a special solution of Eq. (5), the general solution of Eq. (5) can be expressed as  $\dot{\theta} = \dot{\theta}_s + \dot{\theta}_a$ , then there is:

$$\dot{X} = J(\dot{\theta}_s + \dot{\theta}_a) \tag{5}$$

Obtained by formula (5):

$$J\dot{\theta}_a = 0 \tag{6}$$

Given the terminal velocity  $\dot{X}$ , there are infinitely many feasible solutions of joint velocity  $\dot{\theta}$ , which are composed of the special solution  $\dot{\theta}_s$  and the general solution  $\dot{\theta}_a$  of the corresponding homogeneous equations  $J\dot{\theta}_a = 0$ . This means that  $\dot{\theta}_a$  is the element of the zero space  $N(J)$  of Jacobian  $J$ , and all of these solutions constitute the zero space of Jacobian matrix, which is the  $n - m$  dimensional subspace of  $n$  dimensional real space  $R^n$ , denoted as  $N(J)$ . It is orthogonal to row space  $R(J^T)$  of Jacobian matrix. The dimension  $\dim N(J)$  of the zero space represents the arbitrary range of the given terminal velocity of the super redundant manipulator. From the physical point of view, these motions in the joint space will not cause the motion of the end, which is the self motion of the super redundant manipulator [7].

The above process completes the determination of the redundant space of the manipulator, which lays the foundation for the trajectory tracking planning of the manipulator.

### 2.4 The Obstacle Avoidance Index of Manipulator is Selected

The selection of obstacle avoidance indicators will directly affect the effectiveness of obstacle avoidance. Especially for dynamic obstacle avoidance, the random movement of obstacles, choosing a reasonable index that can accurately and quickly describe the position relationship between the obstacle and the manipulator is particularly important for ensuring the real-time nature of obstacle avoidance planning [8].

The traditional distance index needs to calculate the minimum distance from the obstacle to each member, and then take the minimum value. Take three members as an example,  $d_{\min} = \min\{d_1, d_2, d_3\}$ . When the bar is in some special configuration, the perpendicular foot of the minimum distance from the obstacle to the bar may fall on the extension line of the bar. The extension line does not belong to a part of the manipulator, so it is not accurate to calculate it by substituting the minimum distance. In this case, it is necessary to take multiple mark points on the bar and traverse the distance from each mark point to the obstacle. It can be seen that the traditional distance obstacle avoidance index is not accurate enough, but also needs to calculate multiple mark points, which costs a lot of time [9].

In view of the above problems, this paper preselects the minimum distance index  $H_{d-\min}$ , and its idea is: to establish corresponding bounding boxes for different manipulator configurations, use intersection test, eliminate other safety members before calculating the real-time distance, only consider the position relationship between the colliding members and obstacles, and calculate the distance value in the local coordinate system of the members, as shown in Fig. 3.

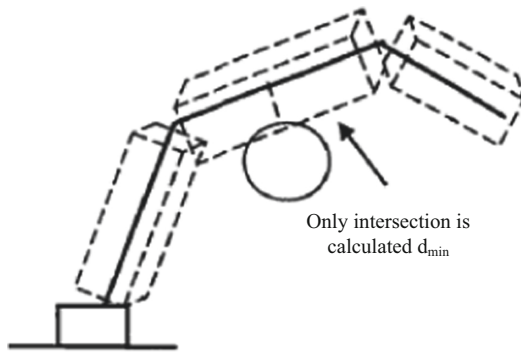


Fig. 3. Pre selected minimum distance Obstacle Avoidance Index

If there are multiple members intersecting in the intersection test, then  $H_{d-\min}$  takes the smallest of the intersection distances.  $H_{d-\min}$  index is used to describe the position relationship between the obstacle and the manipulator. Under the condition of avoiding the vertical foot from the obstacle to the bar falling on the extension line of the bar, the safety bar is removed, the traditional distance calculation is optimized, and the unnecessary amount of calculation is removed. In the process of obstacle avoidance, the larger the  $H_{d-\min}$  is, the better. It means that the farther away from the obstacle, the safer the manipulator is.

## 2.5 Trajectory Tracking Planning for Obstacle Avoidance of Manipulator

After obtaining the real-time minimum distance  $d_{\min}$  based on the above calculation, the trajectory tracking planning is carried out using the escape velocity dynamic

obstacle avoidance algorithm. Equation (4) provides the joint speed required to meet the terminal motion requirements, but if there are obstacles in the working space of the robot arm, one or more links may be too far away from the obstacle when the robot arm is in a certain position. Near or colliding with obstacles. To this end, this article first sets a “threshold” distance. During the movement of the manipulator arm, if the distance between each connecting rod and the obstacle is greater than the “threshold” distance, the position and posture of the manipulator arm can be obtained without changing the minimum norm solution (pseudo-inverse solution). On the contrary, the null space vector should be used to adjust the posture of the manipulator without changing the terminal posture, so as to meet the condition of no obstacles.

If the mechanical arm intersects with the obstacle at a certain time in the process of motion, the collision point between the link and the obstacle is  $x_o$ . In order to make the super redundant manipulator avoid obstacles, zero space vector should be selected, which is the closest point  $x_o$  and has the velocity component  $\dot{x}_o$  far away from the obstacles, so as to prevent the collision between the obstacles and the manipulator. Therefore, there are two basic requirements for obstacle avoidance trajectory tracking planning of super redundant manipulator: the first is to meet the terminal motion requirements, and the second is to avoid moving obstacles [10, 11], namely:

$$\begin{cases} J\dot{\theta} = \dot{X} \\ J_o\dot{\theta} = \dot{x}_o \end{cases} \quad (7)$$

In formula (7),  $\dot{x}_o$  is the set speed to avoid obstacles, and  $J_o$  is the Jacobian matrix of the collision point. Substitute formula (4) into formula (7), and increase the minimum distance  $d_{\min}$  from the obstacle avoidance index  $H_{d-\min}$ .

In order to reduce the influence of rank changes and maintain the continuity of joint speed, the obstacle avoidance gain  $a_n$  and the escape speed  $a_o$  are introduced. The dynamic obstacle avoidance inverse kinematics of the escape speed is expressed as:

$$\dot{\theta} = J^+ \dot{X} + a_n [J_o(I - J^+ J)]^+ (a_o \dot{x}_o - J_o J^+ \dot{X}) \quad (8)$$

In summary, through the introduction of VR technology, the tracking planning of the obstacle avoidance trajectory of the hyper-redundant manipulator is realized, which provides effective support for the application and development of the hyper-redundant manipulator.

### 3 Application Performance Analysis

#### 3.1 Experimental Preparation

For the application performance of the obstacle avoidance trajectory tracking planning method of the super-redundant manipulator based on VR technology, a simulation experiment is designed on the ground experimental system of the super-redundant manipulator based on the air-floating platform.

The ground experimental system of the hyper-redundant manipulator is an important part of the development process of the hyper-redundant manipulator. The ground experimental system based on the hyper-redundant manipulator can simulate a weightless environment, verify the validity of the theory related to the hyper-redundant manipulator, and test the performance and function of the manipulator. In the experimental system:

- 1) Air flotation platform: In order to simulate the microgravity environment in space, this experimental platform is based on the air flotation method, using the jet reaction force of the air bearing to support the seven-degree-of-freedom super-redundant manipulator on a flat and smooth marble platform. Counteract the effects of gravity. The air pump is used as the air source to supply air for each air foot to support the robotic arm to simulate a microgravity environment;
- 2) Central controller: coordinate and control the motion of the robotic arm, send joint commands to each joint controller, and the central controller and each joint controller communicate based on the 1553B bus protocol;
- 3) Ground inspection equipment: Located between the central controller and the simulation notebook, it plays the role of data forwarding, storage, viewing and management. The communication between the central controller and the ground inspection equipment is based on the 1553B bus protocol. The ground inspection equipment and the simulation notebook Communication is based on UDP protocol;
- 4) Simulation Notebook: realize VR technology, simulation and task planning function. At the same time, it communicates with the operator station to collect the operation status and send the sensor data to the operator station, which is based on UDP protocol;
- 5) Console: through the console, the operator sends control commands to check the status of the manipulator, which realizes the good interaction between the operator and the manipulator.

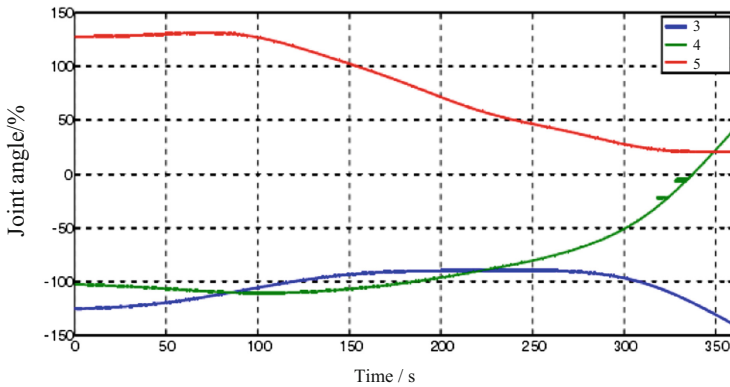
Due to the limitation of the experimental platform, it is difficult to realize the simultaneous motion of seven joints of the 7-DOF super redundant manipulator. The axes of joints 3, 4 and 5 of the 7-DOF super redundant manipulator are parallel to each other, so when joints 1, 2, 6 and 7 are fixed and only the end position of the manipulator is controlled, it is still a super redundant manipulator control problem. It can be used to verify the inverse kinematics and Obstacle Avoidance Trajectory Tracking planning of the super redundant manipulator, but the amount of calculation is less than that of the 7-DOF super redundant manipulator. In the experiment, keeping the angles of joints 1, 2, 6 and 7 at  $0^\circ$ ,  $-180^\circ$ ,  $0^\circ$  and  $90^\circ$ , joints 3, 4 and 5 move, which is equivalent to the motion of planar three-bar super redundant manipulator in plane  $X - Z$ .

Although the 3, 4, and 5 joints of the hyper-redundant manipulator can move within the range of  $[-270^\circ, 270^\circ]$ , due to the limited area of the air bearing table and the restriction of the air foot support mechanism attached to the manipulator, The range of motion of the robotic arm on the experimental platform is limited. In the experiment, the range of motion of joint 3  $[-165^\circ, -90^\circ]$ , the range of motion of joint 4  $[-120^\circ, 120^\circ]$ , the range of motion of joint 5  $[20^\circ, 165^\circ]$ , the joints of joints 3, 4, and 5 The speed cannot exceed  $2^\circ/s$ , and the absolute position accuracy of the end is less than or equal to 10mm.

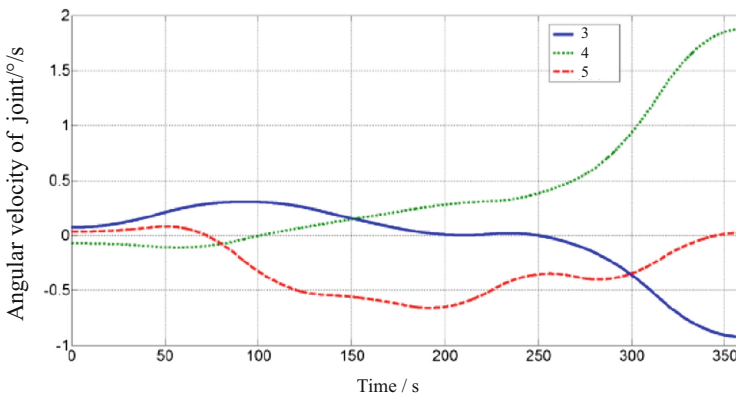
### 3.2 Analysis of Results

Task description: plan a collision free trajectory from the initial configuration to the target configuration, and make the trajectory cost of the end of the manipulator as small as possible. The initial configuration  $[-136.93^\circ, -74.31^\circ$  and  $24.57^\circ]$  and the target configuration  $[-139.92^\circ, 40.68^\circ$  and  $20.57^\circ]$ .

Through the simulation experiment, the change curve of joint angle and velocity in the process of obstacle avoidance movement of super redundant manipulator is obtained, as shown in Fig. 4.



(1) Joint angle curve



(2) Joint angular velocity curve

**Fig. 4.** Curve of joint angle and speed change during obstacle avoidance movement of the robotic arm

Can be seen from the Fig. 4, 3, 4, 5 joints Angle and angular velocity are within the scope of the constraints, and a smooth curve, can be used for the control of mechanical arm, arm successfully avoid the obstacles and reach the target configuration, today's

hyper redundant manipulator trajectory tracking of obstacle avoidance planning requirements, fully demonstrates the effectiveness of the proposed design method.

On this basis, the traditional trajectory tracking planning method based on machine vision technology is compared and further verified from the perspective of timeliness of response of tracking planning instructions. The results are shown in Fig. 5.

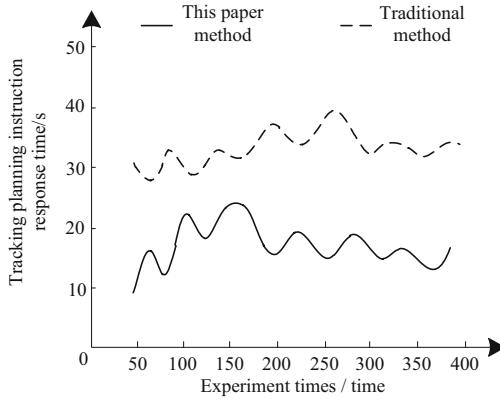


**Fig. 5.** Comparison of response timeliness of tracking planning instructions by different methods

According to Fig. 5, with the increase of verification times, the response time of tracking planning instructions of different methods is also changing constantly. However, it is obvious that the time of the proposed method is lower than that of the traditional method. It can be seen that the method presented in this paper can realize trajectory tracking planning more quickly.

## 4 Conclusion

In this study, VR technology was applied to the obstacle avoidance trajectory tracking planning of hyperredundant manipulator. In the design process, the hyperredundant manipulator is taken as the research object, the virtual model of the hyperredundant manipulator is constructed by using VR technology, and the redundant space of the manipulator is determined. Then, the pre-selected minimum distance index was selected as the obstacle avoidance index of the manipulator. According to the calculated real-time minimum distance, the inverse kinematics equation of the manipulator was obtained by using the escape velocity dynamic obstacle avoidance algorithm, so as to realize the trajectory tracking planning. The experimental results show that this method can effectively meet the requirements of obstacle avoidance trajectory tracking planning for hyperredundant manipulators and is suitable for extensive application. In the following research, the proposed method will be further optimized from the perspective of improving the control accuracy.

**Fund Projects.** Supported by the National Key Research and Development Program of China (No. 2019YFC1408003).

## References

1. Aijuan, L., Wanzhong, Z., Xibo, W., et al.: ACT-R cognitive model based trajectory planning method study for electric vehicle's active obstacle avoidance system. *Energies* **11** (1), 75 (2018)
2. Mu, Z., Liu, T., Xu, W., et al.: A Hybrid Obstacle-avoidance method of spatial hyper-redundant manipulators for servicing in confined space. *Robotica* **37**(6), 998–1019 (2019)
3. Yue, M., Wu, X., Guo, L., et al.: Quintic polynomial-based obstacle avoidance trajectory planning and tracking control framework for tractor-trailer system. *Int. J. Control Autom. Syst.* **17**(10), 2634–2646 (2019)
4. Hu, Z., Zhu, D., Cui, C., et al.: Trajectory tracking and re-planning with model predictive control of autonomous underwater vehicles. *J. Navig.* **72**(2), 321–341 (2019)
5. Kano, H., Fujioka, H.: Spline trajectory planning for road-like path with piecewise linear boundaries allowing double corner points. *Sice J. Control Meas. Syst. Integrat.* **11**(6), 429–437 (2018)
6. Xiuxia, Y., Yi, Z., Weiwei, Z.: Obstacle avoidance method of three-dimensional obstacle spherical cap. *J. Syst. Eng. Electron.* **29**(05), 182–192 (2018)
7. Chiaravalli, D., Califano, F., Biagiotti, L., et al.: Physical-consistent behavior embodied in B-spline curves for robot path planning. *IFAC-PapersOnLine* **51**(22), 306–311 (2018)
8. Liu, S., Liu, D., Srivastava, G., Połap, D., Woźniak, M.: Overview and methods of correlation filter algorithms in object tracking. *Complex Intell. Syst.* **7**(4), 1895–1917 (2020). <https://doi.org/10.1007/s40747-020-00161-4>
9. Liu, S., Lu, M., Li, H., et al.: Prediction of gene expression patterns with generalized linear regression model. *Front. Genet.* **10**, 120 (2019)
10. Liu, S., Bai, W., Zeng, N., et al.: A fast fractal based compression for MRI images. *IEEE Access* **7**, 62412–62420 (2019)
11. Wu, Q., Zhang, C., Zhang, M., et al.: A modified comprehensive learning particle swarm optimizer and its application in cylindricity error evaluation problem. *Int. J. Performabil. Eng.* **15**(3), 2553 (2019)